Sorption-enhanced reforming with limestone from iron production

**Roland Diem · Stefan Mueller · Michael Fuchs ·
Johannes C. Schmid · Hermann Hofbauer**

Abstract In this work, the experimental performance of
sorption-enhanced reforming using limestone as bed material,
which is used in raw iron production, is presented. Steam gasi-
fication of solid biomass by sorption-enhanced reforming pro-
cess (SER) leads to product gas with high hydrogen content and
low tar content. The product gas can be used for a wide range of
applications. This includes heat and electricity production, syn-
thetic fuels, and other downstream processes. On the basis of
dual fluidized bed steam gasification of biomass (dual fluid
gasification), a reactive bed material is used to enhance the
formation of hydrogen. Blast furnaces in iron production operate
on the principle of chemical reduction, whereby carbon monox-
ide and hydrogen reduce the iron to its elemental form. The
present paper summarizes the results of an experimental investi-
gation into SER with limestone usually used as a part of iron
production. The illustrated results reflect the operation of
sorption-enhanced reforming within an experimental facility at
the Vienna University of Technology.

Keywords Biomass · Gasification · Hydrogen · Fluidized
bed · Sorption-enhanced reforming

Abbreviations

DFB	Dual fluidized bed
Nm^3	Cubic meters according to standard conditions for pressure and temperature (0 °C, 1.013 bar)
wt.-%	Percentage by weight
vol.-%	Percentage by volume
SER	Sorption-enhanced reforming
db	Dry basis

R. Diem (✉) · S. Mueller · M. Fuchs · J. C. Schmid · H. Hofbauer
Institute of Chemical Engineering, Vienna University of Technology,
Getreidemarkt 9/166, 1060 Vienna, Austria
e-mail: roland.diem@tuwien.ac.at

1 Introduction

In times of growing concern about greenhouse gasses, energy-
intense industry sectors are looking for renewable energy
sources in order to replace fossil energy sources like coal and
natural gas. Gasification processes are a well-known technolo-
gy for producing a medium calorific gas from biomass. As well
as producing electricity, the produced gas can be used as
feedstock for chemical synthesis. With regard to raw iron
production, the blast furnace process works according to the
counter flow principle where the iron core gets reduced by
reducing agents like carbon monoxide (CO) and hydrogen
(H_2) provided by coal. Dual fluid gasification of biomass can
be used for the generation of product gas with high reduction
potential [1]. This produced gas contains hydrogen (H_2), carbon
monoxide (CO), methane (CH_4), carbon dioxide (CO_2), ethane
(C_2H_6), ethylene (C_2H_4), propane (C_3H_8), water (H_2O), dust,
and tar. Sorption-enhanced reforming (Fig. 1) is operated with
bed materials mainly consisting of calcium (Ca). High hydro-
gen content is reached by a reduction of the CO_2 content due to
a selective transport of CO_2 enabled by the operated bed
material. At the same time, sorption-enhanced reforming leads
to reduced tar content.

The application of sorption-enhanced reforming therefore
leads to an improved product gas composition and can in-
crease the possibilities for product gas utilization. Table 1
shows a comparison of conventional dual fluid gasification
to sorption-enhanced reforming. Conventional dual fluid gas-
ification uses olivine sand as bed material.

Conventional dual fluid gasification reaches a hydrogen
(H_2) content of about 40 vol.-%$_{db}$ [4], whereas sorption-
enhanced reforming with limestone as bed material is able to
exceed concentrations of 60 vol.-%$_{db}$. Previous experimental
results were published, e.g., by Pfeifer et al. [5] and Koppatz
et al. [6]. This paper presents results obtained from experi-
ments with a 100-kW$_{th}$ dual fluid gasifier system using the

Fig. 1 Basic principle of sorption-enhanced reforming [2]
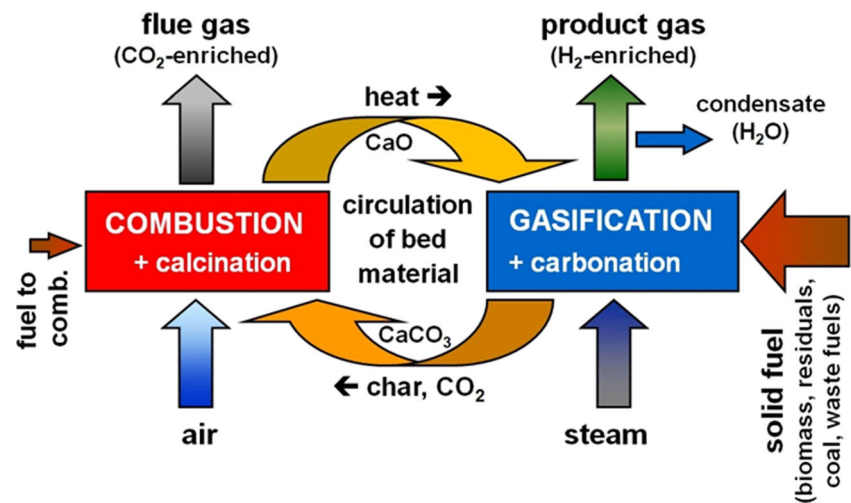
limestone KS_1_09_12 as bed material. The results gained are compared to a similar SER experiment [5]. The limestone material used is used in the iron production process. It is added to the blast furnace to absorb disturbing elements and reduce the melting temperature. Since it is ready on site and available for low costs, the used limestone appears to be a favorable choice. The product gas can be used on site for iron reduction in the blast furnace and as an energy source for auxiliary units. The focus of the presented work is to compare the performance of the used bed material with respect to

- process stability,
- product gas composition,
- bed material loss due to attrition,
- CO_2 transport,
- and process efficiency,

in comparison to data published in literature. The used bed material limestone (KS_1_09_12) came from a quarry and was provided by an actual iron production site in Europe.

2 Methodology and experimental

The experimental setup of the 100-kW$_{th}$ gasifier system at the Vienna University of Technology is presented in Fig. 2. The used dual fluid system combines a steam-blown bubbling fluidized bed gasification reactor and an air-blown fast fluidized bed combustion reactor. Details of the dual fluid concept and the possible process applications are given by Hofbauer et al. [7, 8] and Koppatz et al. [2, 9].

This gasifier system was used to perform SER experiments. The biomass enters the gasification reactor via a screw conveyor directly into the bubbling bed (used feedstock hopper 2). Drying, devolatilizing, gasification, and partial char gasification take place in the bubbling bed. Residual char leaves the

gasification reactor together with bed material through the steam-fluidized lower loop seal toward the combustion reactor.

The combustion reactor (riser) is designed as a highly expanded fluidized bed, a so-called fast bed. Air is used as fluidization agent, which reacts with the residual char serving to heat the bed material by combustion. The system is stabilizing itself since a decrease in the gasification temperature leads to a higher amount of residual char, which results in more fuel for the combustion reactor. In addition to its function as a heat carrier, a selective CO_2 transfer is realized by the bed material limestone $CaO/CaCO_3$ [5]. The carbonation (Eq. (1)) is an exothermic reaction and contributes to the heat demand of the gasification process:

$$CaO_{(s)} + CO_2 \leftrightarrow CaCO_{3(s)} \quad \Delta H^0_{298} = -181 \text{ kJ/mol} \quad (1)$$

Table 1 Product gas composition of conventional gasification of wood pellets compared to sorption-enhanced reforming obtained from experiments with a 100-kW gasifier in Vienna [3]

	Conventional gasification	SER process
Gasification temperature	800–850 °C	600–700 °C
Combustion temperature	900–950 °C	800–900 °C
Bed material	Olivine	Calcite (limestone)
Gasification agent	Steam	Steam
Product gas composition		
H_2 [vol.-%$_{db}$]	36–42	55–75
CO [vol.-%$_{db}$]	19–24	4–11
CO_2 [vol.-%$_{db}$]	20–25	6–20
CH_4 [vol.-%$_{db}$]	9–12	8–14
Tar [g/Nm^3]	4–8	0.3–0.9
Dust [g/Nm^3]	10–20	20–50
H_2O [vol.-%]	30–45	50–65

Fig. 2 Schematic illustration of the used experimental 100-kW$_{th}$ gasifier system [10]
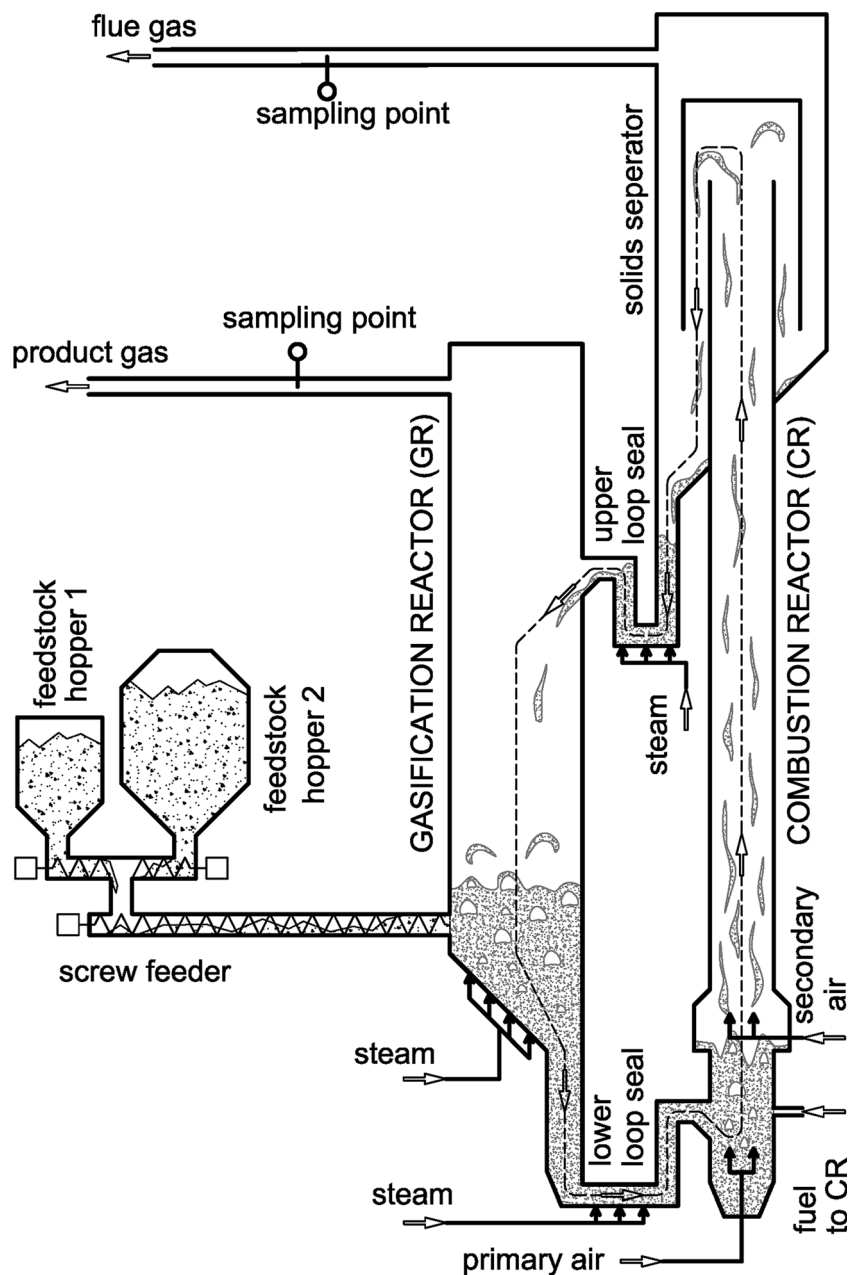
The necessary driving force for the carbonation and calcination is the difference between the CO_2 partial pressure in the reactor and the CO_2 equilibrium partial pressure. The continuous CO_2 removal during the gasification enhances the CO shift reaction (Eq. (2)) toward the desired products, since the change in CO_2 concentration effects a more intensive reaction of H_2O and CO, which leads to a higher concentration of H_2 in the product gas [6].

$$CO + H_2O \leftrightarrow CO_2 + H_2 \; \Delta H^0_{298} = -41 \text{ kJ/mol} \qquad (2)$$

The characteristics of the operated bed material are crucial considering the fluid dynamics and resistance against abrasion. Abrasion leads to a reduced particle size during the operation of solid particles in a fluidized bed, which causes loss of bed material and high dust contents in the flue and product gas. Thus, the requirements on the operated bed material (calcite, limestone) are as follows:

- sufficient CO_2 capacity,
- high carbonation reaction rate,
- good calcination efficiency under specified process conditions,
- good abrasion and attrition resistance,
- catalytic activity toward tar removal,
- and support of the CO shift reaction.

Fig. 3 Mass and temperature change in the thermogravimetric analysis [12]
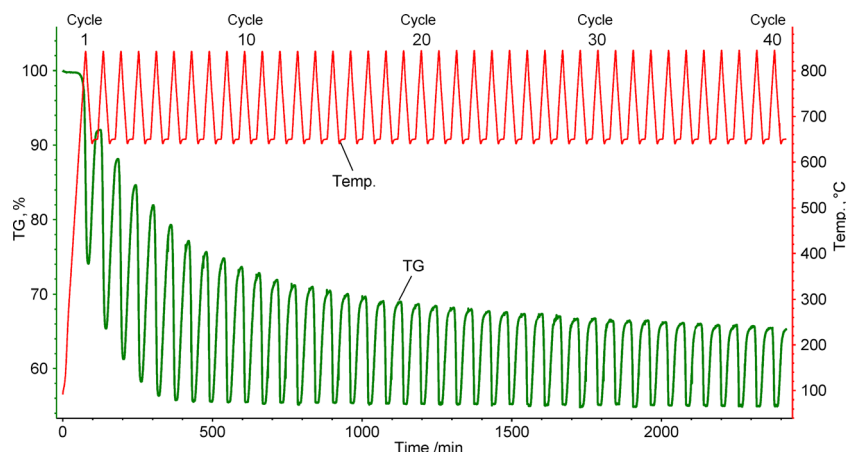
In order to investigate the resistance to attrition of the used bed material, a standard test for the determination of resistance to fragmentation was performed [11]. The bed material (KS_1_09_12) turned out to have a high resistance to fragmentation (residue of 24 wt.-% with a particle diameter >1.6 mm).

The CO_2 load of bed materials based on calcium oxide (CaO) is limited to 1 mol CO_2 per mol CaO. The stated value can only be achieved in theory due to several mechanisms that reduce the effective CO_2 transport [6]. Figure 3 shows the decay of the CO_2 load during a thermogravimetric analysis. The operated temperature change was performed between an upper temperature of 850 °C and a lower temperature of 650 °C with an isothermal hold for 20 min at 650 °C. At the beginning the change of mass, which corresponds to the amount of CO_2 being absorbed, was observed to be 25 wt.-% followed by a decay. Within the first 500 min, a noticeable decrease from 25 to 19 wt.-% change of mass indicates a reduction of the molar transport capacity of CaO particles after eight carbonation-calcination cycles (Table 2) [12]. After 1500 min, the decline of the mass change, and consequently the molar transport capacity, waned to an average value of 11 wt.-% mass change within the last ten cycles. The gas atmosphere used during the thermogravimetric analysis contained the following: 10 vol.-% CO_2, 30 vol.-% H_2O, and 60 vol.-% N_2.

The test campaign aimed to achieve experimental data, operating in a steady state under SER conditions with limestone (KS_1_09_12) as bed material. Figure 4 shows the particle size distribution before and after the experiment. The applied bed material, limestone, had an initial Sauter diameter of d_{SV}=425 μm. Details about the chemical composition of the used bed material are

displayed in Table 3. Table 4 shows operation parameters compared to convventional gasification using olivine as bed material.

In order to provide favorable process conditions, the temperature within the gasifier was kept around T_G=670–680 °C and the temperature within the combustor was kept at the level of about T_C=820–860 °C. During the experiment, online monitoring and data recording of pressures and temperatures were conducted. The gas composition of the flue and product gas was monitored and two tar measurements were carried out.

After the startup procedure, which is characterized by heating up of the reactors, favorable conditions for the sorption-enhanced reforming process were maintained. The analysis of the wood pellets used for the experiment is listed in Table 5. The pellets are cylindrically shaped with a diameter of 6 mm and a mean particle length of 20 mm (DIN51737). After 3 h of steady-state operation and two tar measurements, the test campaign ended with the shutdown procedure. The tar content of the product gas was measured twice during the steady-state operation (Fig. 5).

Tars detectable with a gravimetric method (i.e., molecular weight higher than toluene) were measured as described in literature by Pfeifer et al. [13]. The measuring method was
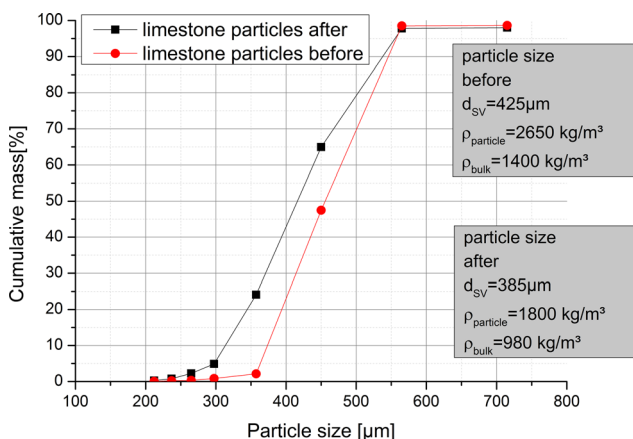
Table 2 CO_2 capacity after thermogravimetric cycles

Thermogravimetric cycles	Cycle 1	Cycle 10	Cycle 20	Cycle 30	Cycle 40
CO_2 load [kg$_{CO2}$/kg$_{KS\_1\_09\_12}$]	0.26	0.18	0.13	0.12	0.10

Fig. 4 Size distribution and properties before and after the experiment

Table 3 Chemical composition of limestone from KS_1_09_12 according to internal standard (GLV = annealing loss)

Limestone KS_1_09_12	[wt.-%]
GLV	44.4
CaO	51.7
MgO	3.6
H_2O	0
Fe_2O_3	0.1
SiO_2	0.1
Al_2O_3	0.1

Table 5 Analysis of wood pellets

	Unit	Dry basis (db)	Raw basis
Water content	[wt.-%]	–	6.57
Ash content	[wt.-%]	0.27	0.25
Carbon	[wt.-%]	50.72	47.32
Hydrogen	[wt.-%]	5.51	5.15
Nitrogen	[wt.-%]	<0.05	<0.05
Sulfur	[wt.-%]	<0.005	<0.005
Chlorine	[wt.-%]	<0.005	<0.005
Volatiles	[wt.-%]	86.3	80.63
Fixed carbon	[wt.-%]	13.7	12.8
Heating value	[MJ/kg]	20.3	18.97
Calorific value	[MJ/kg]	19.1	17.7

developed at the Institute of Chemical Engineering [10] (Vienna University of Technology) and is based on the tar protocol "Gravimetric Tars" developed by Neeft et al. [14].

3 Results

During the experiments, comprehensive data was registered by the process control system.

Data was recorded over the entire operation of 3.5 h. Overall, the recording of data and carrying out of measurements

were conducted to gain results with KS_1_09_12 with respect to the following:

- product gas composition,
- operation parameters,
- mass and energy balances,
- bed material performance,
- and bed material consumption.

Table 4 Typical ranges of operating conditions of the 100-kW$_{th}$ gasifier plant at Vienna University of Technology, conventional gasification [10] compared to SER

Operation parameter	Unit	Conv. DFB gasification	SER (this work)
General			
Bed material particles	–	Olivine	Limestone
Bed material particle density	[kg/m^3]	2850	2650 (1800)[a]
Bed material inventory	[kg]	100	100 (68)[a]
Gasification reactor			
Typical fluidization regime	–	Bubbling bed	Bubbling bed
Steam-to-fuel ratio	[kg$_{H2O}$/kg$_{fuel,db}$]	0.8–1.1	0.7
Thermal power, feed gasifier	[kW]	66–97	73
Temperature, gasifier	[°C]	800–810	670–680
Superficial gas velocity, U	[m/s]	0.41–0.56	0.29–0.32
Fluidization ratio, U/U$_{mf}$	–	2.1–5.6	2.5–4.6
Fluidization ratio, U/U$_t$	–	0.06–0.12	0.06–0.1
Mean gas residence time (bubbling bed)	[s]	0.27–0.37	0.4–0.5
Mean gas residence time (freeboard)	[s]	3–4	5–6
Combustion reactor			
Typical fluidization regime	–	Fast bed	Fast bed
Thermal power, fuel to combustion	[kW]	22–31	7
Temperature, combustion zone	[°C]	840–900	820–860
Superficial gas velocity, U	[m/s]	8.8–10.1	6.9–7.7
Fluidization ratio, U/U$_{mf}$	–	44–100	90–170
Fluidization ratio, U/U$_t$	–	1.3–2.3	2.1–3.5
Mean gas residence time	[s]	0.73–0.85	0.9–1.1

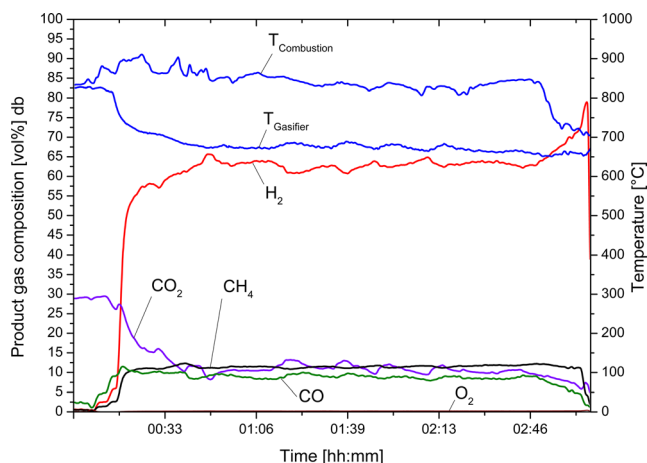[a] Values in brackets according to bed material composition after partial calcination

Fig. 5 Product gas composition, gasification temperature (TG), and combustion temperature (TC) according to the process control system during the experiment with KS_1_09_12

Table 7 Breakdown of GC-MS tar composition with KS_1_09_12

GC-MS components	First measurement [mg/Nm³]	Second measurement [mg/Nm³]
Phenol	1097	1494
Naphthalene	780	763
1H-indene	559	576
Tyrene	387	403
4-Methyl-phenol	350	470
Anthracene	254	245
Acenaphthylene	235	218
2-Methyl-naphthalene	166	180
2-Methyl-phenol	135	175
Fluorene	110	113

The composition of the product gas (Table 6), the gasification temperature, and the temperature in the combustion zone are displayed in Fig. 5. Two product gas samples were taken (Fig. 5) and analyzed with regard to tar and dust (Tables 6 and 7). During the first hours of operation, a temperature gap between the gasifier and combustion reactor had to be regulated in order to achieve SER conditions. Decreasing CO_2 concentration accompanied by increasing H_2 content marks the beginning of favorable SER operation conditions.

Table 7 shows the absolute amount of the gas chromatography-mass spectrometry (GC-MS) components. Phenol is found to be the component with the highest absolute amount.

Table 8 and Fig. 6 summarize achieved product gas composition. Table 9 shows key performances indicators of SER and conventional gasification.Compared to the SER results from Pfeifer et al. [5], tar concentrations have been measured

higher whereas dust content has been measured considerably lower than 22.8 g/Nm³. This might be because of the maintained operation parameters or better characteristics of the bed material. The loss of limestone due to attrition was noticeable from the continuous decrease in the pressure in the bubbling bed. Bed material samples, taken before and after the experiment, showed different particle size distribution (cf. Fig. 4). The initial Sauter diameter of $d_{SV}=425$ μm went down to $d_{SV}=385$ μm. The bed material leaving the gasifier is a mixture of char and calcium oxide particles that are partially carbonated. In addition to the observed decreasing particle size, the rate of attrition was measured by doing a rough mass balance. The average outgoing bed material mass flow was observed to be ~1.6 kg/h.

4 Discussion

The performed test campaign showed that limestone KS_1_09_12 is suitable for sorption-enhanced reforming. Compared to the product gas data of Pfeifer et al. [5], the dust content is considerably lower with the limestone KS_1_09_12. Nevertheless, a significant increase in the dust content comparing the first and second measurements (Fig. 5, Table 6) during the test run is observable. The higher dust

Table 6 Product gas composition of sorption-enhanced reforming with KS_1_09_12

	Unit	First measurement SER KS_1_09_12	Second measurement SER KS_1_09_12
Hydrogen (H_2)	[vol.-%db]	62	63
Carbon monoxide (CO)	[vol.-%db]	9.4	8.7
Carbon dioxide (CO_2)	[vol.-%db]	11.3	11.2
Methane (CH_4)	[vol.-%db]	11.4	11.3
Ethylene (C_2H_4)	[vol.-%db]	1.2	1.2
Dust content	[g/Nm³]	5.53	9.79
Char content	[g/Nm³]	3.66	7.05
Gravimetric tar	[g/Nm³]	2.3	2.35
GC-MS tar	[g/Nm³]	5.01	5.68
Water content	[vol.-%]	51	52

Table 8 Comparison of tar and dust content in the product gasses yielded from test campaigns with different bed materials

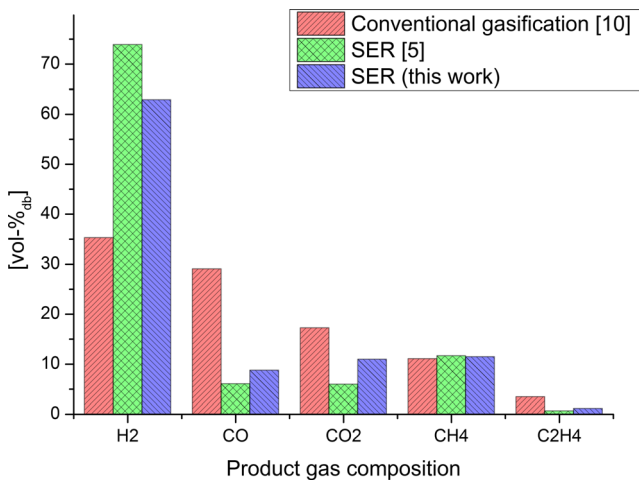|	Unit	Conv. gasific. [10]	SER [5]	SER (this work)
Temperature gasifier	[°C]	802	645	674
Tar content (GC-MS/grav.)	[g/Nm³]	11.7/6.0	–/1.4	5.3/2.3
Dust content	[g/Nm³]	6.5	22.8	7.7
Char content	[g/Nm³]	47.4	28.8	5.4
Water (H_2O)	[vol.-%]	40-55	51.4	63.9

Fig. 6 Comparison of the product gas compositions yielded from test campaigns with different bed materials

CO_2 emission. Coal is a comparably cheap reducing agent that at the same time induces most fossil CO_2 emissions. But low costs for emission allowances at a price level of 20€/t CO_2 still have a low impact on the results. Iron ore reduction through the aid of natural gas or through a reducing agent from sorption-enhanced reforming achieves quite similar operation costs per year [1]. A parameter analysis shows that SER for raw iron production is favorable from an economic point of view if

- the wood chip price is lower than 54€/t_{atro} (12€/MWh),
- the natural gas price is higher than 29€/MWh,
- or the coal price is higher than 26€/MWh [1].

content might be due to the abrasion of the bed material, which increases over time. Compared to Pfeifer [5], the bed material shows a comparatively good abrasion resistance, but in terms of the dust content, it is important to note the longer operation time of Pfeifer [5]. With regard to the char content, an increase over time is observable. The reason for this appears to be an accumulation of char inside the reactor due to an incomplete combustion of the char particles inside the combustion reactor. Furthermore, higher tar content compared to that of Pfeifer's [5] is observed, which probably results from lower catalytic activity of limestone concerning tar cracking reactions in comparison to the calcite used by Pfeifer [5]. In order to make a statement on bed material and process characteristics, which are crucial for a good sorption-enhanced reforming performance, further sampling points would help. An overall economic analysis showed that, compared to traditional sources of reducing agents in the iron-making industry such as coal and natural gas, hydrogen from biomass through SER offers a process option with reduced fossil

5 Conclusion and outlook

The experiment showed that KS_1_09_12 can be used well as bed material. Sorption-enhanced reforming is a promising process for gaining hydrogen-rich product gas. The experimental operation of sorption-enhanced reforming with limestone (KS_1_09_12) from an iron production site leads to a favorable product gas composition for iron ore reduction. Dual fluidized bed gasification under sorption-enhanced reforming conditions is a possible way to integrate renewable feedstock into the iron production process. The tar content was quantified to about 5.3 g/Nm³ GC-MS, 2.3 g/Nm³ gravimetric tar. In order to keep the total bed material inventory of a dual fluid gasification system constant, the outgoing mass flow of bed material has to be compensated for by fresh bed material. Lost bed material due to abrasion effects could be reused within the iron-making process because limestone is already used as an important additive for iron ore reduction in the blast furnace. Since the used pilot plant is not laid out for sorption-enhanced reforming, certain design criteria should be considered. Sorption-enhanced reforming needs a certain temperature gap between the two reactors. Hot bed material, in particular CaO, coming from the combustion reactor should not exceed a certain temperature. If the temperature in the gasification reactor gets too high, the carbonation reaction Eq. (1) stops [6]. For future reactor designs aimed at operating sorption-enhanced reforming, it would be advisable to introduce a cooling unit in the upper loop seal. With such a cooling unit, it would be possible to withdraw a certain amount of heat and ensure favorable SER conditions. Nevertheless, experiments by Hawthorne et al. [15], Pfeifer et al. [5], and also Soukup et al. [3] reached hydrogen (H_2) contents above 70 vol.-%$_{db}$ in the product gas. It is assumed that experiments using limestone KS_1_09_12 with lower temperatures in the gasification reactor would also reach such high hydrogen contents.

Table 9 Sorption-enhanced reforming compared to typical results of conventional dual fluid gasification

Operation parameter	Unit	Conv. gasific. [4, 10]	SER (this work)
Relative water conversion rate	[kg$_{H2O}$/kg$_{fuel}$]	0.07–0.14	0.23
Absolute water conversion rate	[kg$_{H2O}$/kg$_{H2O}$]	0.09–0.16	0.25
Cold gas efficiency (100 kW test plant)	[%]	50–55	58
Estimated cold gas efficiency (indus. plants)	[%]	70–75	70–80
Logarithmic deviation from CO-Shift eq.	–	(−0.3)–(0.5)	(−0.37)
Lower heating value of product gas	[MJ/Nm³]	12–14	13.6

Further experimental campaigns are planned using the next generation of dual fluid gasifier [16, 17] including improved solid separator systems for reduced bed material consumption.

References

1. Mueller S (2013) Hydrogen from biomass for industry—industrial application of hydrogen production based on dual fluid gasification. Dissertation, Vienna University of Technology
2. Koppatz S, Mueller S, Schmid J (2012) Future energy technology. Vienna University of Technology, ISBN 978-3-9502754-3-8
3. Soukup G, Pfeifer C, Kreuzeder A, Hofbauer H (2009) In situ CO_2 capture in a dual fluidized bed biomass steam gasifier—bed material and fuel variation. Chem Eng Technol 32(3):348–354. doi:10.1002/ceat.200800559
4. Koppatz S, Schmid J, Pfeifer C, Hofbauer H (2012) The effect of bed particle inventories with different particle sizes in a dual fluidized bed pilot plant for biomass steam gasification. Ind Eng Chem Res 51(31): 10492–10502. doi:10.1021/ie202353b
5. Pfeifer C, Puchner B, Hofbauer H (2009) Comparison of dual fluidized bed steam gasification of biomass with and without selective transport of CO_2. Chem Eng Sci 64(23):5073–5083. doi:10.1016/j.ces.2009.08.014
6. Koppatz S, Pfeifer C, Rauch R, Hofbauer H, Marquard-Moellenstedt T, Specht M (2009) H2 rich product gas by steam gasification of biomass with in situ CO_2 absorption in a dual fluidized bed system of 8MW fuel input. Fuel Process Technol 90(7–8):914–921. doi:10.1016/j.fuproc.2009.03.016

7. Hofbauer H, Veronik G, Fleck T, Rauch R (1997) The FICB—gasification process. In: Bridgewater A (ed) Developments in thermochemical biomass conversion, vol 1. Kluwer, London
8. Hofbauer H, Loeffler G, Kaiser S, Fercher E, Tremmel H (2002) Six years experience with the FICB-gasification process. In: 12th conference on biomass and bioenergy, Amsterdam
9. Koppatz S, Pfeifer C, Hofbauer H (2011) Comparison of the performance behavior of silica sand and olivine in a dual fluidized bed reactor system for steam gasification of biomass at pilot plant scale. Chem Eng J 175:468–483. doi:10.1016/j.cej.2011.09.071
10. Schmid J, Wolfesberger U, Koppatz S, Pfeifer C, Hofbauer H (2012) Variation of feedstock in a dual fluidized bed steam gasifier—influence on product gas, tar content, and composition. Environ Prog Sust Energ 31(2):205–215. doi:10.1002/ep.11607
11. Standardization ECF (2013) Tests for mechanical and physical properties of aggregates. Part 2: methods for the determination of resistance to fragmentation, vol EN 1097–2
12. Sobotka C (2013) Bestimmung der CO_2 Aufnahmekapazität von vier Kalksorten mittels TG Analyse STA 449 F3 inkl. Wasserverdampfer. Report, University of Leoben, Department of Nonferrous Metallurygy, Leoben
13. Pfeifer C, Puchner B, Hofbauer H (2007) In-situ CO2-absorption in a dual fluidized bed biomass gasifier to produce a hydrogen rich syngas. Int J Chem React Eng 5(1):1542–6580. doi:10.2202/1542-6580.1395
14. Neeft J.P.A. et al. (1999) Guideline for sampling an analysis of tar and particles in biomass producer gas. In: Progress in thermochemical biomass conversion, pp 162–175
15. Hawthorne C et al (2012) Operation and results of a 200-Kw_th dual fluidized bed pilot plant gasifier with adsorption-enhanced reforming. Biomass Convers Biorefinery 2(3):217–227. doi:10.1007/s13399-012-0053-3
16. Schmid J, Proell T, Kitzler H, Pfeifer C, Hofbauer H (2012) Cold flow model investigations of the countercurrent flow of a dual circulating fluidized bed gasifier. Biomass Convers Biorefinery 2(3):229–244. doi:10.1007/s13399-012-0035-5
17. Hofbauer H, Schmid J, Fuchs J (2012) Cold flow model study of an advanced dual fluid bed system for fuel conversion. In: 3rd international symposium on gasification and its application (iSGA-3), 2012, Vancouver, British Columbia, Canada